Geographic variability in the export of moist static energy and vertical motion profiles in the tropical Pacific

L. E. Back[1] and C. S. Bretherton[1]

[1] Column-integrated moist static energy (MSE) budgets were calculated using daily data from three reanalyses (1998–2001) and ISCCP radiative cooling. The MSE export by the circulation was separated into vertical and horizontal MSE advection components in order to examine how observationally-derived vertical motion profiles affect gross moist stability calculations. In a 2000 km-wide region in the central-eastern Pacific ITCZ, vertical motions import MSE, implying a negative gross moist stability. Horizontal MSE advection is negative and of similar magnitude to vertical MSE advection in rainy regions. Geographic differences in export of MSE by the vertical circulation are primarily due to differences in the shape of the vertical motion profile. In the west Pacific warm pool rainy regions, mean horizontal convergence extends up to 300 mb, while in parts of the Pacific ITCZ where meridional SST gradients are strong, the vertical motion profile is bottom-heavy, with convergence below 800 mb and divergence above. On daily timescales, the mode of vertical motion variability has little dependence on precipitation rate and is consistent with observed regional differences in the vertical structure of TRMM PR reflectivities. **Citation:** Back, L. E., and C. S. Bretherton (2006), Geographic variability in the export of moist static energy and vertical motion profiles in the tropical Pacific, *Geophys. Res. Lett.*, *33*, L17810, doi:10.1029/2006GL026672.

1. Introduction

[2] Many theories about the interaction of the large-scale tropical circulation with deep moist convection have been based on assuming the system is adequately described by a single mode of vertical velocity variability. These include two-layer models [e.g., *Gill*, 1980] and continuous models in which large-scale baroclinic motions have a single vertical structure [e.g., *Neelin and Zeng*, 2000]. Such models have also been thought to provide a satisfying explanation why the observed wave speeds [*Wheeler and Kiladis*, 1999] of convectively-coupled equatorial waves match the speeds predicted by shallow water theory with an equivalent depth of about 25 meters [*Neelin and Yu*, 1994; *Emanuel et al.*, 1994; *Yu and Neelin*, 1997].

[3] Consistently representing the interaction of cumulus convection with the large-scale circulation in such models requires consideration of moisture as well as temperature, so they are usefully phrased using moist static energy (MSE). MSE is approximately conserved following air parcels, even as they undergo phase changes between vapor and liquid

including precipitation processes. Atmospheric convection vertically rearranges MSE, but does not affect the column-integrated MSE:

$$MSE = C_p T + Lq + gz \tag{1}$$

where T is temperature, q is the mixing ratio of water vapor, z is height, C_p is the specific heat of air, L is the latent heat of evaporation, and g is gravitational acceleration.

[4] The equivalent depth that MSE-based models predict is proportional to an effective stability in deep convective regions, the gross moist stability, M [*Neelin and Held*, 1987], which is derived by consideration of column-integrated MSE budgets. The gross moist stability measures the ratio of MSE exported from a tropospheric column by the mean circulation per unit of mean upward mass flux. In the context of MSE-based models, M controls the sensitivity of the convective rainfall to forcing by other terms in the MSE budget. M has typically been defined in linearized models by assuming one vertical mode of variability in the divergent circulation. For instance, in variations on the Quasi-equilibrium Tropical Circulation Model (QTCM [*Neelin and Zeng*, 2000])

$$M(x,y) = \int_{p_0}^{p_t} \frac{\partial h(x,y,p)}{\partial p} \Omega(p) dp, \tag{2}$$

where h is the MSE, p_0 is the surface and p_t is the tropopause height and $\Omega(p)$ is a structure function for vertical pressure-velocity, defined positive, which is weighted slightly toward the upper troposphere.

[5] *Yu et al.* [1998] looked at climatological gross moist stability variations across the tropics using the QTCM-specified profile adjusted to match a local maximum depth of convection and found small positive values of M in regions of active convection, consistent with QTCM assumptions. However, we will find that the actual vertical motion profile is vastly different than the QTCM-assumed $\Omega(p)$ in parts of the ITCZ. In fact, one geographically-invariant, scaled $\Omega(p)$ is not sufficient to describe geographic variations in the vertical motion profile. This has important consequences for gross moist stability as a conceptual tool and for QTCM-like unimodal models in general.

[6] There has been little exploration of MSE budgets and thinking using observationally-derived vertical motion profiles, $\omega(x, y, p)$. In fact, an unambiguous definition of a quantity like gross moist stability that accounts for the vertical structure of ω has only recently been proposed [*Bretherton et al.*, 2006]. Hence, while this study is inspired by ideas about gross moist stability, we find it more illuminating to look directly at the column-integrated export of MSE by tropical circulations and do not try to explicitly compute a gross moist stability.

[1]Department of Atmospheric Sciences, University of Washington, Seattle, Washington, USA.

[7] Using reanalyses, we study the export of moist static energy by vertical and horizontal motions in the tropical Pacific and find that there is a 2000 km wide region in the ITCZ where vertical circulations likely import MSE, corresponding to negative gross moist stability. In this region, export of column-MSE by vertical motions is not providing a limit on the amount of convection. In fact, in parts of this region, the entire advective contribution to the column, including horizontal advection and transients, appears to be close to zero. This challenges the adequacy of a single gross moist stability for understanding convective-coupled wave speeds and ITCZ structure over the equatorial Pacific Ocean.

2. Data Description

[8] We use three independent reanalysis datasets to compute time-mean column integrated moist static energy budgets for 1998–2001. From the Data Support Section of the National Center for Atmospheric Research (NCAR), we obtained ECMWF 40 year reanalysis (ERA40, 23 pressure levels, 2.5° grid [*Uppala et al.*, 2005]) temperature, wind speeds, humidity, surface latent and sensible heat fluxes. From the Climate Diagnostics Center (URL: http://www.cdc.noaa.gov), we also obtained comparable NCEP-NCAR reanalysis data (17 pressure levels, 2.5° grid [*Kalnay et al.*, 1996]) and NCEP/DOE AMIP-II-reanalysis data (NCEP2 [*Kanamitsu et al.*, 2002]). The computation of time-mean MSE budgets from this data has substantial errors and uncertainties, so the reanalyses are treated as three independent estimates for all computations. We expect that results which are consistent in all three reanalyses are fairly robust, since the reanalyses use widely differing parameterizations.

[9] At each pressure level archived in each reanalysis, storage, horizontal advection and vertical advection were computed, corresponding to the first four terms in the budget equation for MSE (h):

$$\frac{\partial h}{\partial t} = -\left(u\frac{\partial h}{\partial x} + v\frac{\partial h}{\partial y} + \omega\frac{\partial h}{\partial p}\right) + g\frac{\partial}{\partial p}\left[F_{turb}^h + F_{rad}\right] + S_h \quad (3)$$

[10] The fifth and sixth terms describe turbulent transport of h and the radiative flux divergence, respectively. S_h includes small source terms due to the nonconservation of h in moist thermodynamic processes, particularly involving ice. We vertically integrated equation 3 from 1000 mb to 100 mb, assuming no top-of-atmosphere turbulent fluxes (brackets indicate mass-weighted vertical integrals of storage, horizontal and vertical advection):

$$\left\langle\frac{\partial h}{\partial t}\right\rangle = \left\langle -u\frac{\partial h}{\partial x} - v\frac{\partial h}{\partial y}\right\rangle + \left\langle -\omega\frac{\partial h}{\partial p}\right\rangle + F_{turb}^h(0) + \Delta F_{rad} + R_h$$
$$(4)$$

[11] We also extracted surface MSE fluxes $F_{turb}^h(0)$ from the reanalyses. *Jiang et al.* [2005] compared reanalysis turbulent surface heat fluxes to Tropical Atmosphere-Ocean (TAO) buoys; in their analysis, NCEP-NCAR has the smallest mean bias of -6 W/m^2, ERA40 bias is -16 W/m^2 and NCEP2 bias is -28 W/m^2. All biases vary greatly with location and time. R_h is a residual due to vertically-averaged source terms $\langle S_h\rangle$, discretization errors due to the limited

resolution of the reanalysis output, and mean drifts of the model from reality. The vertically integrated budget terms were computed using daily mean winds and thermodynamic fields, as well as using monthly mean winds and thermodynamic fields. As shown in Section 3, in the regions of interest, these two realizations are very similar. The difference between these two approaches is ascribed to transient variability resolved within the reanalyses. Column-integrated radiative cooling estimates were computed from International Satellite Cloud Climatology Project (ISCCP [*Rossow and Schiffer*, 1999]) monthly surface and top-of-atmosphere radiative flux estimates. *Cronin et al.* [2006] showed the surface radiative flux estimates using this dataset agree much better with TAO observations than do the reanalyses.

[12] The horizontal and vertical MSE advection terms are shown separately because in theoretical studies of equatorial wave dynamics [e.g., *Neelin and Yu*, 1994; *Yano and Emanuel*, 1991; *Mapes*, 2000], horizontal advection has often been neglected by linearizing the governing equations about a horizontally uniform mean state and only vertical advection considered. In addition, it is the vertical MSE advection that is most comparable to gross moist stability as defined in equation (2).

[13] In a fully consistent budget, R_h would be small compared to the dominant budget terms. However in our analysis, R_h is non-negligible and has geographic variability in the time-mean, as well as between reanalyses. We further discuss this issue in the results section.

[14] *Trenberth et al.* [2002] studied numerical errors associated with computing moist static energy budgets from data which has been interpolated to pressure coordinates, as we have done. When using pressure coordinates, errors are substantial over land and at latitudes higher than 30 degrees, but within the region we examine in this study, we find that differences between reanalyses are substantially larger than errors shown in Trenberth's work, so we conclude that our datasets are suitable for this study. *Trenberth and Stepaniak* [2003] also computed the "divergent energy transport" using model level NCEP data from 1979–2001, which is equivalent to the sum of the vertical and horizontal advection we show. The sum of our calculated horizontal and vertical advection terms is broadly consistent with Trenberth's Figure 4, providing further evidence that our approach to computing MSE export is reasonable.

[15] We also obtained vertical motion profiles from simulations using three major atmospheric general circulation models (AGCMs) forced by seasonally-varying sea surface temperatures: the National Center for Atmospheric Research (NCAR) Community Atmosphere Model (CAM) 3.0, the Geophysical Fluid Dynamics Laboratory (GFDL) Atmospheric Model (AM) 2.12b, and the NASA Global Modeling and Assimilation Office (GMAO) NSIPP-2 model. Details on these simulations are given by *Wyant et al.* [2006].

3. Results

[16] Figure 1 shows annually-averaged horizontal, vertical and total column MSE advection over the tropical Pacific computed from the monthly mean fields of the two reanalyses. The red curves bound rainy regions with annual-mean reanalysis-predicted rainfall exceeding 3.5 mm/day in ERA40 and NCEP-NCAR, corresponding
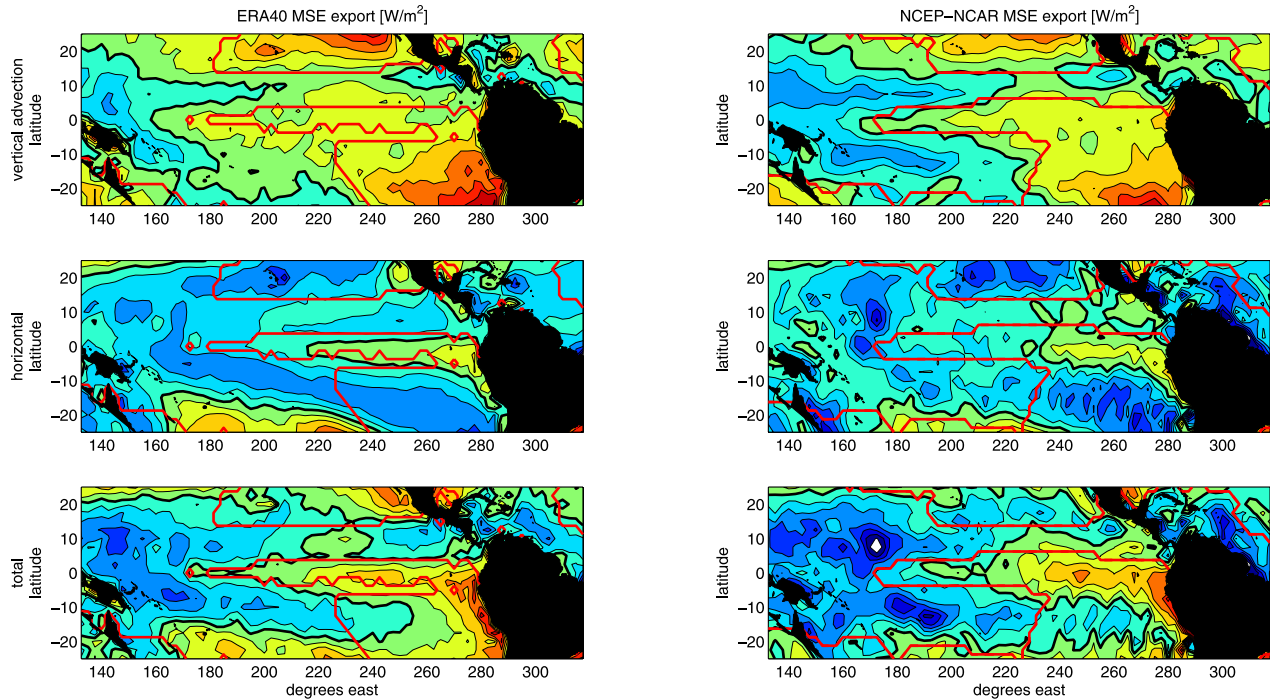
Figure 1. Export of moist static energy associated with (top) vertical and (middle) horizontal and (bottom) total circulation in reanalyses. (left) Budget terms computed from ERA40 and (right) NCEP-NCAR. Heavy black line is zero contour, other black contours every 25 W/m², where lighter shading (or bluer colors) indicates more export. White (or red) dashed contour shows 3.5 mm/day precipitation.

roughly to regions in which precipitation exceeds the evaporation and horizontal advective drying, implying mean moisture convergence and upward motion. The NCEP2 reanalysis MSE advection results share most relevant features with NCEP-NCAR or ERA40 and are omitted due to space considerations. In most of the west Pacific, vertical advection tends to export moist static energy in rainy regions, but in all of the reanalyses, there is a substantial region in the ITCZ around 120–140°W where the vertical circulation imports moist static energy. In fact, even the total advective export of MSE in this region, including horizontal advection, is close to zero. Horizontal MSE advection is almost universally negative in the rainy regions, reflecting mean horizontal dry and cold advection into these humid areas of warm SST. Horizontal MSE advection is comparable to vertical advection throughout most of the rainy region.

[17] To further illuminate the zonal structure of the MSE export and study the role of transients, Figure 2 shows cross sections at 7.5–10 °N (the mean latitude of the Pacific ITCZ) of the components of MSE advection computed using daily reanalysis fields. Figure 2 also shows net MSE export by transients, defined as the difference between the calculated daily advection terms and the terms calculated using monthly mean reanalysis fields. The transient horizontal and vertical advection is small. Including transients in Figure 1 produces almost indistinguishable results (not shown).

[18] Figure 2d shows the sum of the remaining MSE budget terms, evaporation and radiation. Residuals in the calculated MSE budget are shown in Figure 2e. In all reanalyses, there tends to be a more negative residual in

the west Pacific than in the east Pacific, implying column inconsistencies between the MSE advection and the diabatic MSE source. This tendency is small in ERA40 compared to the NCEP reanalyses.

[19] Differences in column-integrated vertical MSE advection can be associated with differences in the MSE profile and/or differences in the vertical velocity profile. Vertical advection of MSE can also be expressed by integration by parts and mass continuity as $\langle -h(\partial u/\partial x + \partial v/\partial y)\rangle$, which involves cancelation between convergence of moisture at low levels where vertical velocity is increasing with height, and divergence of potentially warm air (high dry static energy) at levels where the convection detrains. For example, both more low-level moisture or more horizontal wind convergence can increase vertical advective export.

[20] Figure 3 shows selected examples of mean MSE and vertical velocities over regions in the west Pacific warm pool (gridpoints centered 140–160°E, 5–7.5°N) and the east Pacific ITCZ (gridpoints centered 120–140° W, 7.5–10°N) where the vertical circulation imports MSE. The MSE profile looks similar at the two locations and throughout the Pacific ITCZ; the differences in vertical velocity profiles are far more striking. In the west Pacific, the mean MSE of the detraining air is much higher than the mean MSE of converging air. In the east Pacific, however, detrainment begins near 800 mb, so the MSE of the detraining air is lower than that of the converging air. As these examples illustrate, differences in vertical velocity profiles are the main factor determining the magnitude and sign of vertical MSE advection. Figures 3c and 3d show that three SST-forced AGCMs (described by *Wyant et al.*
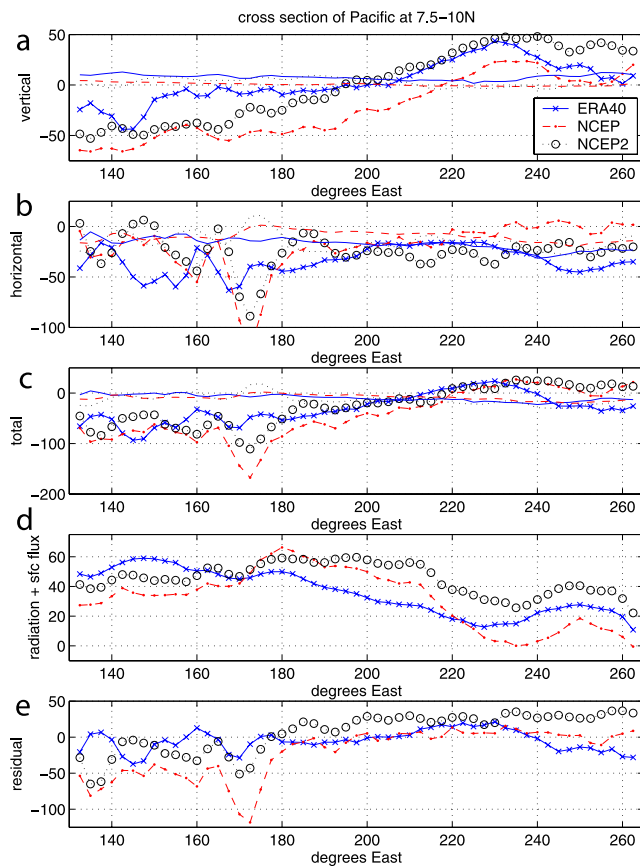
Figure 2. Cross sections at 7.5–10N of export of moist static energy associated with (a) vertical, (b) horizontal, (c) total circulation, as well as (d) sum of radiative flux divergence and surface fluxes and (e) budget residual. Lines with symbols are terms computed from daily-mean fields, and lines without symbols are "transients" (daily minus monthly terms). All radiative cooling is computed from ISCPP FD data.
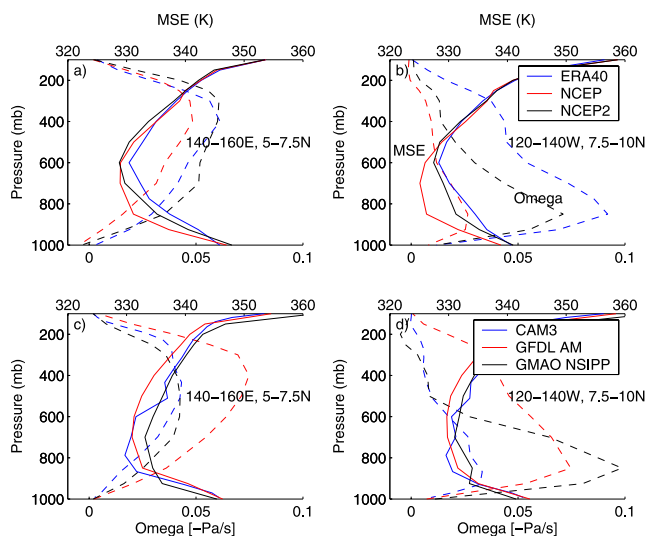

Figure 3. Mean vertical motion and moist static energy profiles in selected regions in Pacific ITCZ. (a and b) Computed from reanalyses and (c and d) computed from atmospheric GCMs.
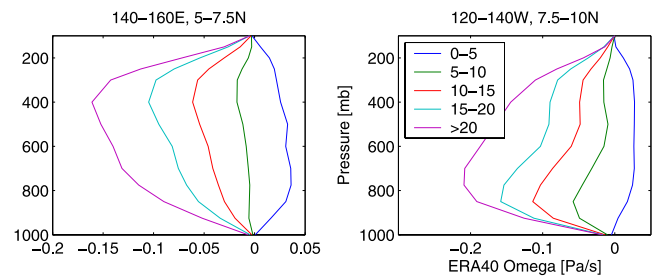

Figure 4. ERA40 vertical motion profiles binned by precipitation [mm/day] in same regions as previous figure.

[2006]) have qualitatively similar vertical motion profiles to the reanalyses, which suggests that the contrast in vertical motion profiles between the E and W Pacific rainy regions is robust to inter-model differences.

[21] One may ask whether the mode of ω variability changes with the amount of convection. For example, does the shallow vertical circulation in the east Pacific, shown in Figure 3, tend to be deeper and export more MSE when there is more rainfall? To test this question, Figure 4 shows a typical example of daily vertical motion profiles binned by daily precipitation. Throughout the reanalyses, as in this example (the same ERA40 east and west Pacific points from Figure 3), the vertical mode of ω variability in a given location has little dependence on precipitation amount, but does vary substantially geographically. Hence, the modulations of MSE transport by transients such as convectively-coupled waves appear to behave similarly to the mean, and also correspond to negative gross moist stability in the east Pacific ITCZ in contrast to common theoretical assumptions.

[22] Mean vertical motion in the deep tropics is directly tied to apparent diabatic heating, which in turn is dominated in rainy regions by "latent" heating (broadly defined to include vertical turbulent heat fluxes). *Schumacher et al.* [2004] used a precipitation and stratiform rain fraction climatology from the Tropical Rainfall Measurement Mission (TRMM) Precipitation Radar (PR) to derive latent heating profiles across the tropics, which are in apparent contradiction to the reanalyzed ω-profiles presented here (see their Figure 4). However, their analysis used geographically-invariant specified stratiform and convective latent heating profiles and thus includes only variability associated with differences in stratiform rain fraction. Differences in storm height and distribution of latent heating within a convective or stratiform column were not considered. The reanalysis results suggest that these factors are critically important. Figure S1[1] shows a cross-section plot of the ratio of mean PR-retrieved reflectivity at 6 km to 2 km, an indirect measure of the shape of the latent heating profile. This ratio is much higher in the west Pacific, indicating elevated latent heating, than in the east Pacific, and tracks the "top-heaviness" of the reanalyzed ω-profiles quite convincingly.

[23] We have documented the substantial variability in mean vertical velocity in deep convective regions, but have thus far not touched on what may control this shape. Dynamical control through frictionally driven boundary layer convergence associated with SST gradients has been

---

[1]Auxiliary materials are available in the HTML. doi:10.1029/2006GL026672.

proposed as a control on the location of the ITCZ. In the model of *Lindzen and Nigam* [1987] temperature gradients within the boundary layer, controlled by sea-surface temperature variations, drive associated pressure gradients which can force strong boundary-layer convergence. This mechanism may drive predominantly bottom-heavy convection in regions with strong meridional SST gradients like the east-central Pacific. This is supported by the results shown in Figure 3 that three major AGCMs robustly predict the difference in east versus west Pacific ω profiles, despite their diverse moist physics parameterizations. By adding a simple boundary layer to the QTCM, *Sobel and Neelin* [2006] can also reproduce the influence of SST-forced frictional convergence on changing the vertical structure of ω in an idealized ITCZ. The MSE framework should be fruitful for further analysis of the thermodynamic implications of ω bottom-heaviness in the central Pacific ITCZ.

References

Bretherton, C. S., P. N. Blossey, and M. E. Peters (2006), Comparison of simple and cloud-resolving models of moist convection-radiation interaction with a mock-Walker circulation, *Theor. Comput. Fluid. Dyn.*, in press.

Cronin, M. F., N. A. Bond, C. W. Fairall, and R. A. Weller (2006), Surface cloud forcing in the east Pacific stratus deck/cold tongue/ITCZ complex, *J. Clim.*, 19, 392–409.

Emanuel, K. A., J. D. Neelin, and C. S. Bretherton (1994), On large-scale circulations in convecting atmospheres, *Q. J. R. Meteorol. Soc.*, 120, 1111–1143.

Gill, A. E. (1980), Some simple solutions for heat-induced tropical circulation, *Q. J. R. Meteorol. Soc.*, 106, 447–462.

Jiang, C.-L., M. F. Cronin, K. A. Kelly, and L. Thompson (2005), Evaluation of a hybrid satellite and NWP based turbulent heat flux product using TAO buoys, *J. Geophys. Res.*, 110, C09007, doi:10.1029/2004JC002824.

Kalnay, E., et al. (1996), The NCEP/NCAR 40-year reanalysis project, *Bull. Am. Meteorol. Soc.*, 77, 437–471.

Kanamitsu, M., W. Ebisuzaki, J. Woollen, S.-K. Yang, J. J. Hnilo, M. Fiorino, and G. L. Potter (2002), NCEP-DOE AMIP-II reanalysis (R-2), *Bull. Am. Meteorol. Soc.*, 83, 1631–1643.

Lindzen, R. S., and S. Nigam (1987), On the role of sea surface temperature gradients in forcing low-level winds and convergence in the tropics, *J. Atmos. Sci.*, 44, 2418–2436.

Mapes, B. E. (2000), Convective inhibition, subgrid-scale triggering energy, and stratiform instability in a toy tropical wave model, *J. Atmos. Sci.*, 57, 1515–1535.

Neelin, J. D., and I. M. Held (1987), Modeling tropical convergence based on the moist static energy budget, *Mon. Weather Rev.*, 115, 3–12.

Neelin, J. D., and J.-Y. Yu (1994), Modes of tropical variability under convective adjustment and the Madden-Julian oscillation, Part I: Analytical theory, *J. Atmos. Sci.*, 51, 1876–1894.

Neelin, J. D., and N. Zeng (2000), A quasi-equilibrium tropical circulation model—Formulation, *J. Atmos. Sci.*, 57, 1741–1766.

Rossow, W. B., and R. A. Schiffer (1999), Advances in understanding clouds from ISCCP, *Bull. Am. Meteorol. Soc.*, 80, 2261–2288.

Schumacher, C., R. A. Houze Jr., and I. Kraucunas (2004), The tropical dynamical response to latent heating estimates derived from the TRMM precipitation radar, *J. Atmos. Sci.*, 61, 1341–1358.

Sobel, A. H., and J. D. Neelin (2006), The boundary layer contribution to intertropical convergence zones in the quasi-equilibrium tropical circulation model framework, *Theor. Comput. Fluid. Dyn.*, in press.

Trenberth, K. E., and D. P. Stepaniak (2003), Seamless poleward atmospheric energy transports and implications for the Hadley circulation, *J. Clim.*, 16, 3705–3721.

Trenberth, K. E., D. P. Stepaniak, and J. M. Caron (2002), Accuracy of atmospheric energy budgets from analyses, *J. Clim.*, 15, 3343–3360.

Uppala, S. M., et al. (2005), The ERA-40 re-analysis, *Q. J. R. Meteorol. Soc.*, 131, 2961–3012.

Wheeler, M., and G. N. Kiladis (1999), Convectively coupled equatorial waves: Analysis of clouds and temperature in the wavenumber-frequency domain, *J. Atmos. Sci.*, 56, 374–399.

Wyant, M. C., C. S. Bretherton, J. T. Bacmeister, J. T. Kiehl, I. M. Held, M. Zhao, S. A. Klein, and B. A. Soden (2006), A comparison of tropical cloud properties and responses in GCMs using mid-tropospheric vertical velocity, *Clim. Dyn.*, 27, 261–279.

Yano, J., and K. Emanuel (1991), An improved model of the equatorial troposphere and its coupling with the stratosphere, *J. Atmos. Sci.*, 48, 377–389.

Yu, J.-Y., and J. D. Neelin (1997), Analytic approximations for moist convectively adjusted regions, *J. Atmos. Sci.*, 54, 1054–1063.

Yu, J.-Y., C. Chou, and J. D. Neelin (1998), Estimating the gross moist stability of the tropical Atmosphere, *J. Atmos. Sci.*, 55, 1354–1372.

———————————

L. E. Back and C. S. Bretherton, Department of Atmospheric Sciences, University of Washington, Box 351640, Seattle, WA 98103, USA. (larissa@atmos.washington.edu)